Cent. Eur. J. Phys. • 10(2) • 2012 • 500-505
DOI: 10.2478/s11534-011-0109-1

VERSITA

Central European Journal of **Physics**

Growth and EPR properties of $KSm(WO_4)_2$ and $KEr(WO_4)_2$ single crystals*

Research Article

Grzegorz Leniec[1], Tomasz Skibiński[1†], Slawomir M. Kaczmarek[1], Przemyslaw Iwanowski[2], Marek Berkowski[2]

1 *Institute of Physics, Faculty of Mechanical Engineering and Mechatronics, West Pomeranian University of Technology, Al. Piastow 48, 70-311 Szczecin, Poland*

2 *Institute of Physics, Polish Academy of Sciences, Al. Lotnikow 32/46, 02-668 Warsaw, Poland*

Received 23 September 2011; accepted 14 November 2011

Abstract: Growth conditions and electron paramagnetic resonance investigations of two well oriented $KSm(WO_4)_2$ and $KEr(WO_4)_2$ single crystals have been presented and discussed. Hyperfine structure of Sm^{3+} ion was detected and analyzed for angular and temperature dependences. EPR spectra of $KEr(WO_4)_2$ and its angular dependence showed the presence of 5 magnetically nonequivalent Er centers in the crystal. A change in the type of magnetic interactions was analyzed using mixed (Gaussian and Lorentzian) fits of the EPR spectra.

PACS (2008): 42., 42.55.-f, 42.70.-a

Keywords: EPR • samarium • erbium • single crystal

1. Introduction

Alkaline rare-earth double tungstates have low local symmetry, strong magnetic anisotropy, strong spin-lattice coupling and low-dimensional magnetic structure [1–3]. The potassium-erbium/samarium double tungstate ($KEr(WO_4)_2 \equiv$ KEW and $KSm(WO_4)_2 \equiv$ KSW) crystallize in α-$KY(WO_4)_2$ structure in monoclinic space group $C_{2h}^6 - C2/c$ with cell parameters: KEW: a=10.7287 Å, b=10.5083 Å, c=7.6268 Å, β=130.788°, V=651.026 Å^3, KSW: a=10.6155 Å, b=10.3133 Å, c=7.5363 Å, β=130.750°, V=625.058 Å^3 [2]. This structure is characteristic for several others rare earth double tungstates and belongs to the chain-layered systems. The erbium/samarium ion is surrounded by eight oxygen ions and it is placed on the C_2 point-symmetry site. Their local symmetry and magnetic properties were analyzed in [1, 4]. Because of the low symmetry of single crystals, many physical properties are highly anisotropic. For C_{2h}^6 symmetry, double refraction and pleochroism are expected [5]. The unit cell of KEW/KSW crystal is shown in Fig. 1 [6]. In this paper we present studies of temperature and angular dependences of the EPR spectra of KEW and KSW single crystals. The shapes of these spectra allow

*presented at the 3rd International Workshop on Advanced Spectroscopy and Optical Materials, July 17-22, 2011, Gdańsk, Poland

†E-mail: tocorro@gmail.com

us to find the dominant kind of magnetic interactions between samarium ions in KSW and erbium ions in KEW.

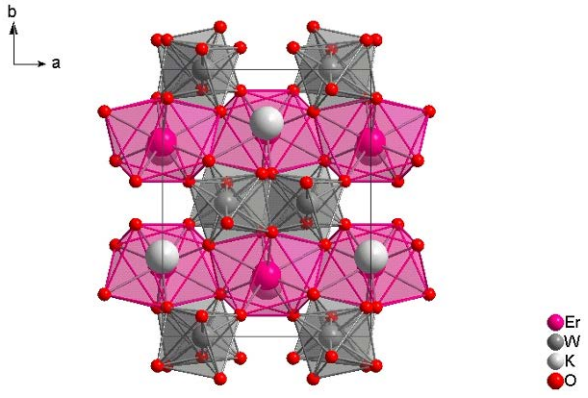

Figure 1. Unit cell of KEW/KSW crystal [6].

2. Experimental setup

Single crystals of KSW and KEW were grown by the Top Seeded Solution Growth (TSSG) method using $K_2W_2O_7$ solvent containing up to 25% mol of crystallized compounds. Structure analysis of obtained crystals was performed at room temperature by X-Ray powder diffraction using Siemens D5000 diffractometer with Ni-filtered Cu Kα radiation. Data was collected in the angle range $20° < 2\theta < 144°$, with a step of 0.02° and averaging time of 10 s/step. The powder diffraction patterns were analyzed by the Rietveld refinement method using DBWS-9807 program [7]. EPR spectra were recorded on a conventional X-band Bruker ELEXSYS E 500 CW-spectrometer operating at 9.5 GHz with 100 kHz magnetic field modulation. The first derivative of the powder absorption spectra has been recorded as a function of the applied magnetic field. Temperature and angular dependences of the EPR spectra of the samples in the temperature range of 4-300 K were recorded using an Oxford Instruments ESP nitrogen-flow cryostat. The crystals were mounted in a resonance chamber and rotated around three perpendicular axes related to crystallographic directions: *a*, *b* and c^*, where c^* axis in monoclinic and $KRE(WO_4)_2$[1] system is perpendicular to *a*- and *b*- crystallographic directions. The Sm^{3+} ion spin Hamiltonian in KSW contains Zeeman and hyperfine interaction terms. For the Er^{3+} ion in KEW, the term related to hyperfine interactions can be discarded from the spin Hamiltonian because they were not observed in EPR spectra. The spin Hamiltonian for both ions can be described by the following equation :

$$H_s = \mu_B B g S' + S' A I \qquad (1)$$

where S' is an effective spin (S'=1/2), B - the external magnetic field and μ_B - the Bohr magneton. S and I are the electron and nuclear spins of the paramagnetic centres, respectively.
To calculate the spin Hamiltonian parameters, EPR-NMR program was used [8].

3. Results and discussion

3.1. Growth conditions

The $K_2W_2O_7$ solvent is a eutectic composition of the K_2O-WO_3 system. The starting solution for growth process was prepared from high purity materials: K_2CO_3 (5N), WO_3 (4N), Sm_2O_3 (5N) and Er_2O_3 (4N) respectively in a 50x50mm platinum crucible, with 1 mm thick walls. The mixture was melted and homogenized by keeping the solution at a temperature of 30°C above seeding temperature for about 32 h. The seeding temperatures were about 920°C for KSW and 860°C for KEW, measured on the surface of the solution. The vertical and the radial gradients inside the solution were about 0.5 K/mm and about 0.2 K/mm, respectively. The starting cooling rate was 0.05 K/h and it has been then subsequently increased up to 0.3 K/h in order to obtain the required crystal diameter. Growing crystals were pulled up at a rate of 1.2 - 1.5 mm/day. Growing crystals were rotated at 25 rpm at the beginning of the growth process and then the rotation rate was lowered with increasing diameter to 6 rpm. After the growth process the crystals were pulled out from the solution and cooled down to room temperature at the rate of 15 K/h [2].

3.2. EPR properties of KEW single crystal

Erbium has six stable isotopes ^{162}Er, ^{164}Er, ^{166}Er, ^{167}Er, ^{168}Er, ^{170}Er [9]. A Characteristic feature of the EPR spectrum of Er-doped KYW crystal is a strong central line (from the even Er isotopes â€Ş I=0, no nuclear magnetic moments, natural abundance 77.06%) and the eight weak lines corresponding to hyperfine transitions (from ^{167}Er isotopes I = 7/2, natural abundance 22.94%). In crystals with small concentration of Er^{3+} ions one central and 8 hyperfine lines are observed. In dense magnetic systems hyperfine lines may not be visible. Previous studies

[1] *RE means rare earth*

showed also that number of lines in EPR spectrum related to Er^{3+} ions depends on host material, for example in $RbTiOPO_4$ doped with Er^{3+} there are six lines [3]. Fig. 2 shows a temperature dependence of the EPR spectra of KEW crystal in the temperature range of 3.1 - 39.9 K. Each line is relatively broad and it is a superposition of at least five lines (numbered as 1, 2, 3, 4 and 5 - see table 1) related to five magnetically non-equivalent centers. All lines are attributed to Er^{3+} ions with effective spin S'=1/2.

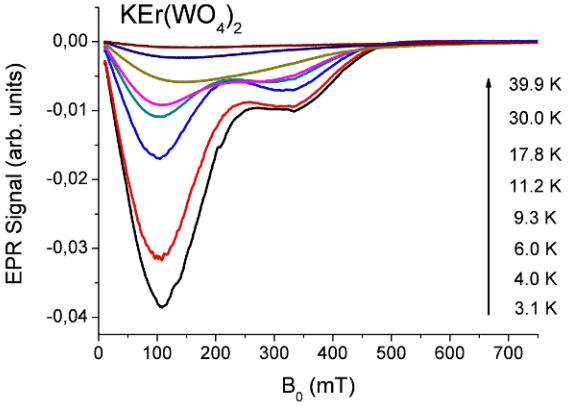

Figure 2. Selected EPR spectra of KEW crystal in the temperature range 3.1 - 39.9 K.

Asymmetric shape of the EPR lines is expected when the paramagnetic dopant is introduced at high concentration. The dipolar and exchange interactions affects the resonance condition. Analysis of the resonance line shows that the type of magnetic interactions is strongly affected by temperature.

The contribution of either dipolar or exchange interactions can be deduced from the shape of the EPR lines. As it is shown in Fig. 3, the shape of the line changes from purely Gaussian (dipolar interactions) to Lorentzian one (exchange interactions). A nearly linear change of Lorentz contribution in the temperature range from 5 K to 25 K, is observed . The linewidths of 1, 2 and 3 centers, are approximately constant (~50 mT) in the measured temperature range, indicating a lack of, or very weak, ferromagnetic interactions. The integral intensity of the EPR lines for centers numbered as 1, 2 and 3 decrease with increasing temperature. This indicates a lack of magnetic interactions or very weak ferromagnetic interactions too. Curie-Weiss fits with Curie-Weiss temperatures: 0.16 K, 1.34 K, 1.67 K for centers numbered 1, 2 and 3, respectively show, that these centers are magnetically equivalent. Centers numbered 4 and 5 change with temperature

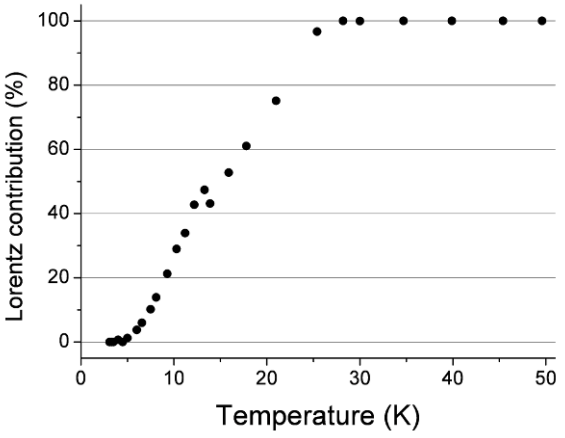

Figure 3. Contributions of Lorentz and Gauss lines into EPR spectra. Zero on the vertical scale means that the line is Gaussian in shape.

much stronger than other centers. The width of line No. 4 in the temperature range 3.1 - 20 K initially rises from ~120 mT to ~220 mT and reaches its maximum, then slightly drops. The width of line No. 5 slightly varies below 20 K and at higher temperatures broadens attaining its maximum at 45 K. This might indicate exchange interactions between erbium ions. Above 20 K, the integrated intensity and linewidth of center No. 4 decrease and exhibit a behavior similar to centers No. 1, 2, 3. The increasing width of line No. 5 might by related to a change in type of the magnetic interactions, from dipolar to exchange interactions and indicates a shortening of the spin-lattice relaxation time. The Bleaney-Bowers and Curie-Weiss fits for centers numbered 4 and 5, show that the exchange constant for the center No. 4 is $2J = 13.45$ K and for the center No. 5 is $2J = 27.73$ K. So, magnetic interactions for centers No. 4 and 5 are ferromagnetic like. Figure 4 presents temperature dependence of overall integral intensity in the KEW single crystal. The fit is given by the following equation:

$$y = \frac{C_1}{x - T_{BB}} \cdot \frac{1-\rho}{1 + 0.3 \cdot e^{\frac{-2J}{x}}} + \frac{\rho \cdot C_2}{x - T_{CW}}, \qquad (2)$$

where: C_1, C_2 are parameters, ρ is the contribution of CW term , T_{BB} the Bleaney-Bowers temperature, T_{CW} the Curie-Weiss temperature and J the exchange interaction constant .

Table 1 presents the spin Hamiltonian parameters (eq. 1) derived from the dependence of the resonance lines position on the rotation angle for KEW (see Fig. 5). The relationship between the resonance line position and the angle of crystal rotation, known as EPR â€IJroadmapâ€{

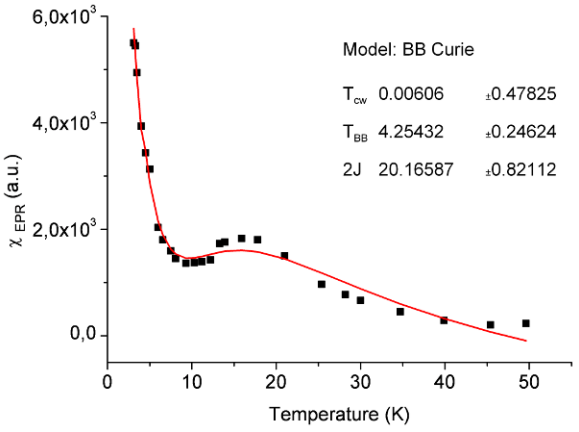

Figure 4. The overall integral intensity of the KEW EPR spectra; solid line represents Bleaney-Bowers fitting; $T_{CW} = 0.00606 \pm 0.47825$, $T_{BB} = 4.25432 \pm 0.24624$, $2J = 20.16587 \pm 0.82112$.

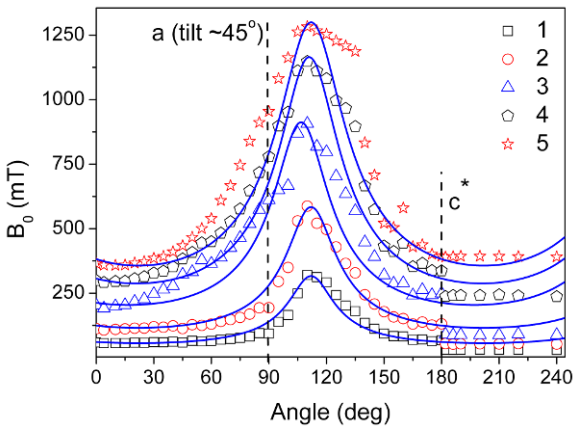

Figure 5. EPR "roadmap" of $KEr(WO_4)_2$ single crystal. Combined data of rotation around *a* and c^* axes. Number 1-5 represents magnetic centers. Solid lines are the results of fitting by EPR-NMR program.

Table 1. Values of the g factor (g_x,g_y,g_z) for five lines contributing to the overall EPR spectra of $KEr(WO_4)_2$ single crystal. Values of g_i in directions x, y, z were acquired by usage of EPR-NMR program.

Center number	g_x	g_y	g_z
1	11.96	1.99	10.24
2	5.86	1.12	4.01
3	3.31	0.64	2.27
4	2.35	0.57	1.58
5	1.90	0.51	1.28

gives information about the local symmetry of magnetic sites and their principal axes of spatial orientation.

3.3. EPR properties of KSW single crystal

The trivalent Sm^{3+} ion has a $4f^5$ electronic configuration with a ${}^6H_{5/2}$ ground multiplet. The low symmetry crystal field splits the ground multiplet into the three Kramers doublets. The nearest excited state ${}^6H_{7/2}$ is located about 1000 cm^{-1} above the ground state [10]. The EPR spectrum observed on the lowest Kramers doublet represents the complex superposition of three spectra. This effect is caused by the fact that samarium has several isotopes with different nuclear moments. For all even isotopes, the nuclear moment is equal to zero and the natural abundance is 71%. The 147 isotope has a natural abundance of 15.07%, a nuclear magnetic moment of 0.8074 μI and a nuclear spin of $I = 7/2$ and the 145 isotope has a natural abundance of 13.82% a magnetic moment of 0.665 μI and a nuclear spin of $I = 7/2$ [11]. Fig. 6 presents the temperature dependence of EPR spectra for KSW single crystal. Clear hyperfine structure originating from two groups of 8 lines coming from two odd isotopes is observed. Because of the strong anisotropy, the complete spectrum can only be observed in the *z* orientation where the *g*-factor is maximal [11].

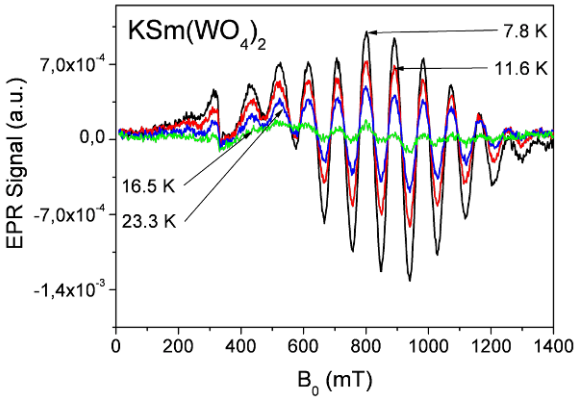

Figure 6. Temperature dependence of EPR spectrum for $KSm(WO_4)_2$ single crystal.

The overall integral intensity of the lines reveals a Curie-Weiss temperature equal to 2.1 K, indicating ferromagnetic interactions between samarium ions in KSW crystal (Fig. 7).

For crystals with strong anisotropy, sample rotation results in strong shift of observed EPR lines. The example of such shift caused by rotation around c^*-axis, at T=7 K

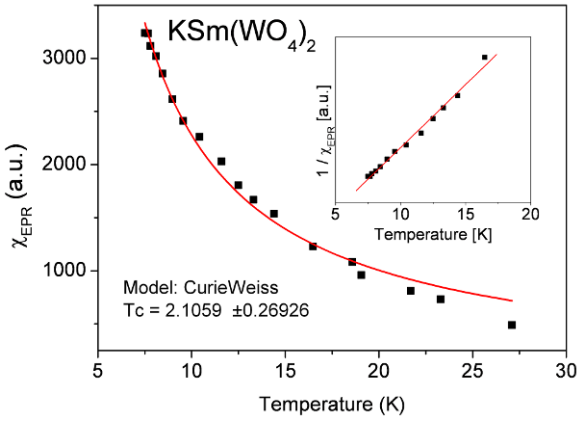

Figure 7. The overall integral intensity of EPR signal for KSW crystal. Solid line marks Curie-Weiss law. In the inset reciprocal of the integral intensity is shown.

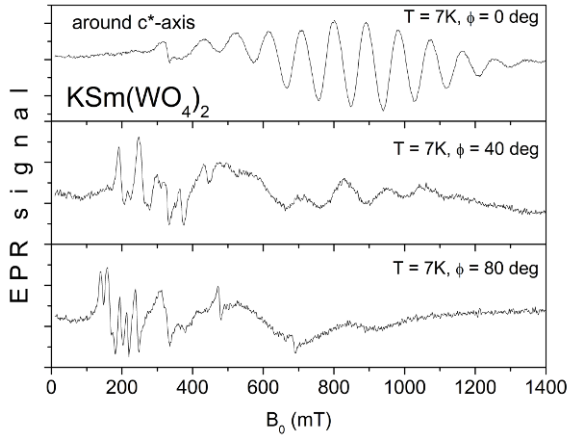

Figure 8. A shift of the KSW EPR lines under rotation around c*-axis: 0, 40 and 80°, at T=7 K.

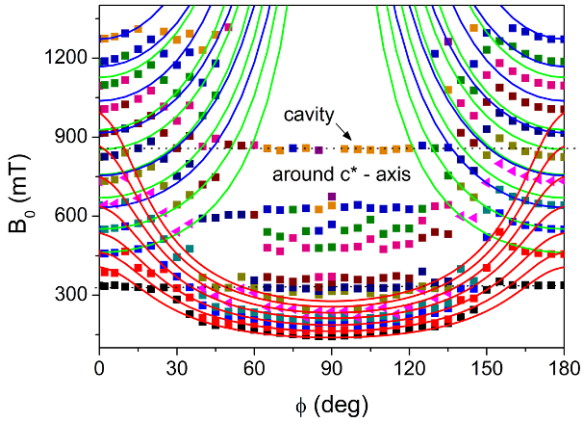

Figure 9. The angular dependence of the EPR lines of the monoclinic Sm^{3+} in the *ab* plane. Squares: experimental data points. The theoretical curves (solid lines) were obtained by using EPR-NMR program.

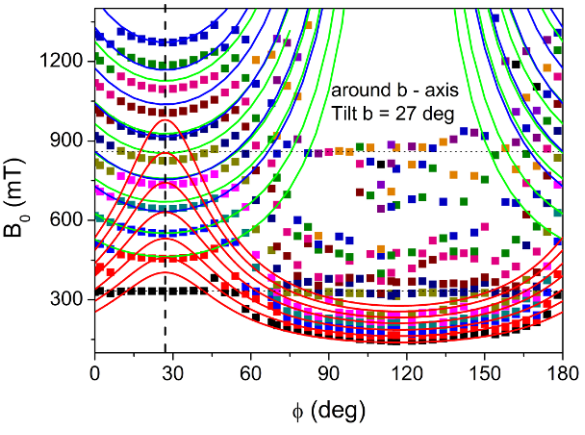

Figure 10. The angular dependence of the EPR lines of the monoclinic Sm^{3+} in the *ac** plane. Squares: experimental data points. The theoretical curves (solid lines) were obtained by using EPR-NMR program.

and three angles: 0, 40 and 80°. is presented in Fig. 8. Full rotation range for two orientations of the KSW crystal (rotation around c^* and b axes) was analyzed. The results of this analysis are presented in Figs. 9 and 10. Clear angular dependence for the monoclinic Sm^{3+} in *ab* and *ac** planes are observed [12]. Different lines (8+8) belonging to 145 and 147 isotopes of samarium are visible. Moreover a 27° tilt is found between y and b axes. Spin Hamiltonian parameters derived using EPR-NMR program are collected in Table 2.

4. Conclusions

It was found that the structure of both crystals under investigation belongs to $C2/c$ space symmetry. Determined lattice parameters are a=10.7287 Å, b=10.5083 Å, c=7.6268 Å, β=130.788°, V=651.026 Å^3 for KEW and a=10.6155 Å, b=10.3133 Å, c=7.5363 Å, β=130.750°, V=625.058 Å^3 for KSW. Optimal conditions for crystal growth by TSSG method were found. The vertical and radial gradients inside the solution should be about 0.5 K/mm and 0.2 K/mm for KSW and KEW, respectively. The starting cooling rate of 0.05 K/h should be subsequently

Table 2. Spin Hamiltonian parameters for $KSm(WO_4)_2$ single crystal (equation 1)

g_x	g_y	g_z	A_x (mT)	A_y (mT)	A_z (mT)
1.49	0.267	0.267	87.1	~0	~0
1.09	0.267	0.267	90.3	~0	~0

increased up to 0.3 K/h in order to obtain the required crystal diameter. Best results were obtained with pulling rate of 1.2 - 1.5 mm/day and rotation speed of 25 rpm at the beginning and then lowered with increasing diameter to 6 rpm. The EPR spectra of KEW crystal showed complex magnetic interactions between the erbium ions. The dipolar and exchange interactions affected the resonance condition. The strength of the exchange interactions defined by the constant of exchange interaction ($2J$) reached the maximum at 20 K. Also resonance conditions were affected strongly by temperature. Below 25 K, dipolar interactions prevailed. At higher temperatures exchange interactions were dominant. Spin Hamiltonian parameters for five recognized erbium centers were determined on the basis of the angular dependence of EPR spectra. Three of them are magnetically equivalent. The others show complex magnetic behaviour. The obtained results very well agree with magnetization measurments reported in [13]. For the KSW crystal, clear hyperfine structure originating from two groups of 8 lines coming from two odd isotopes (145, 147) in the EPR spectra was observed. The spectra indicated a strong anisotropy. Spin Hamiltonian parameters were derived from the angular dependence of the spectra. Both measured crystals revealed positive values of Curie-Weiss temperature, which suggest that ferromagnetic interactions prevail.

References

[1] T. Zayarnyuk et al., P. Soc. Photo-Opt Ins. 5136, 109 (2002)
[2] P. Iwanowski, V. Domukhovski, R. Diduszko, M. Berkowski, Cryst. Res. Technol. 45, 1237 (2010)
[3] U. Griebner, J. Liu, S. Rivier, A. Aznar, R. Grunwald, R.M. Solé, M. Aguiló, F. Díaz, V. Petrov, IEEEJ. QuantumElectron. 41, 408 (2005)
[4] M. T. Borowiec, A. A. Prochorov, A. D. Prochorov, V. P. Dyakonov, H. Szymczak, J. Phys. Condens. Mat. 15, 5113 (2003)
[5] L. Macalik, P. J. Deren, J. Hanuza, W. Strek, A. A. Demidovich, A. N. Kuzmin, J. Mol. Struct. 450, 179 (1998)
[6] V. L. Bekenev, O. Y. Khyzhun, V. V. Atuchin, J. Alloy. Compd. 485, 51 (2009)
[7] E. Mosiniewicz-Szablewska et al., Physica B 296, 369 (2001)
[8] M. J. Mombourquette, J. A. Weil, D. G. McGavin, EPR-NMR User's Manual, Department of Chemistry, University of Saskatchewan (Saskatoon, SK, Canada, 1999)
[9] T.-L. Chang, M.-T. Zhao, W.-J. Li, J. Wang, Q.-Y. Qian, Int. J. Mass Spectrom. 177, 131 (1998)
[10] K. N. R. Taylor, M. I. Darbi, Physics of rare earth solids (Chapman and Hall Ltd., London, 1972)
[11] M. T. Borowiec, A. D. Prokhorov, V. P. Dyakonov, V. I. Kamenev, A. A. Prokhorov, P. Aleshkevych, T. Zayarnyuk, H. Szymczak, Phys. Status Solidi B 246, 1105 (2009)
[12] M. Falin, H. Bill, D. Lovy, J. Phys. Condens. Mat. 16, 1293 (2004)
[13] M. T. Borowiec et al., J. Phys. Condens. Mat. 19, 056206 (2007)